Resonant search for the X17 boson at PADME

Luc Darmé,[1,*] Marco Mancini,[2,†] Enrico Nardi,[3,‡] and Mauro Raggi[4,§]

[1]*Institut de Physique des 2 Infinis de Lyon (IP2I), UMR5822, CNRS/IN2P3, F-69622 Villeurbanne Cedex, France*

[2]*Dipartimento di Fisica, Università di Roma "Tor Vergata," and INFN sezione di Roma "Tor Vergata", 00133 Rome, Italy*

[3]*Istituto Nazionale di Fisica Nucleare, Laboratori Nazionali di Frascati, C.P. 13, 00044 Frascati, Italy*

[4]*Dipartimento di Fisica, Università di Roma La Sapienza and INFN, Sezione di Roma, I-00185 Rome, Italy*

(Received 3 October 2022; accepted 28 November 2022; published 29 December 2022)

We discuss the experimental reach of the Frascati PADME experiment in searching for new light bosons via their resonant production in positron annihilation on fixed target atomic electrons. A scan in the mass range around 17 MeV will thoroughly probe the particle physics interpretation of the anomaly observed by the ATOMKI nuclear physics experiment. In particular, for the case of a spin-1 boson, the viable parameter space can be fully covered in a few months of data taking.

DOI: 10.1103/PhysRevD.106.115036

I. INTRODUCTION

Nuclear excited states with typical energies up to several MeV can source in their transition to the ground state new light bosons with MeV masses. Searches for signals of new physics (NP) of this type are carried out, for example, at the ATOMKI Institute for Nuclear Research in Debrecen (Hungary), which recently reported an anomaly in the angular correlation spectra in ^{8}Be and ^{4}He nuclear transitions [1–3]. The excesses in both spectra can be interpreted as the production and subsequent decay into an $e^\pm$ pair of a new boson, which was named X_{17} after the fitted value of its mass:

$$M_X = \begin{cases} 16.70 \pm 0.35 \pm 0.50\ \text{MeV} & (^8\text{Be}\,[1]), \\ 17.01 \pm 0.16\ \text{MeV} & (^8\text{Be}\,[2]), \\ 16.94 \pm 0.12 \pm 0.21\ \text{MeV} & (^4\text{He}\,[3]), \end{cases} \quad (1)$$

where in the first and third result the first error is statistical and the second is systematic. In order to reproduce the strength of the observed excess, a significant coupling to the quarks is required, along with a coupling to $e^\pm$ that is sufficiently large to allow for the $X_{17} \to e^+e^-$ decays to occur within the ATOMKI apparatus. The nuclear data are not sufficient to fully determine the X_{17} spin/parity quantum numbers [4–6], with the favored possibilities being a vector or a pseudoscalar particle.

The dominant constraints on a particle with such couplings arise from the process $\pi^0 \to \gamma X_{17}$ (followed by $X_{17} \to e^+e^-$), which has been thoroughly explored by the NA48/2 Collaboration [7]. These constraints imply that the couplings of the X_{17} to matter must include a certain amount of pion phobia [5,8,9]. A large number of search strategies based primarily on the X_{17}-quark interactions have been put forward recently; however, in general, they tend to suffer from a large model dependence [10–16]. Owing to its electron-positron interactions, the X_{17} must abide with the standard search for "visible" dark photon, and strong lower bounds on its coupling to electrons arise in particular from the E141 [17–20] and Orsay [21,22] experiments, and more recently from the results of the NA64 Collaboration [23,24]. The visible search from the KLOE experiment [25] finally gives an upper limit at the per-mill level for the coupling to electrons. Covering the remaining allowed parameter space can provide a definite answer regarding the NP origin of the anomaly, and various experimental proposals could probe this region in the future [26–28]. Additional strong indirect bounds can also be obtained under mild theoretical assumptions. In particular, requiring that in the UV limit the X_{17} interactions respect weak $SU(2)$ invariance implies additional constraints, particularly from neutrinos measurements; see, for instance, Refs. [16,29–32].

This paper is devoted to describing a dedicated search strategy for a light bosonic state with a mass of around 17 MeV, based on its production via *resonant* annihilation

*l.darme@ip2i.in2p3.fr
†mancinima@lnf.infn.it
‡enrico.nardi@lnf.infn.it
§mauro.raggi@roma1.infn.it

of positrons from the Frascati Beam Test Facility (BTF) [33] beam on atomic electrons in a fixed target $e^+e^- \to X_{17}$, with a subsequent prompt decay $X_{17} \to e^+e^-$. The importance of the resonant production process, and the possibility of exploiting it in fixed target experiments that exploit a primary positron beam, was first pointed out in Ref. [34]. The importance of this process was later recognized also for electron and proton beam dump experiments, where positrons are produced in electromagnetic showers as secondary particles and led to reanalysis of old results, and improved projections for planned experiments [35–40].

Our search strategy relies on an upgraded version of the Positron Annihilation into Dark Matter Experiment (PADME) experiment [41,42] that is currently running at the Frascati National Laboratories (LNF). PADME exploits a positron beam from the DAΦNE LINAC accelerator in fixed target configuration with an active polycrystalline diamond target of 100 μm. We will discuss in Sec. II the $e^+e^- \to X_{17}$ production mechanism, followed by prompt $X_{17} \to e^+e^-$ decay. The planned Run III of PADME that will be dedicated to search for the X_{17} is described in Sec. III. A quantitative study of the expected sources of background is presented in Sec. IV, and in Sec. V is used to infer projected limits.

II. RESONANT X_{17} PRODUCTION

Let us first consider the case where X_{17} is a spin-1 boson, which interacts with the Standard Model via the following Lagrangian:

$$\mathcal{L}^{\text{Vect.}} \supset \sum_{f=e,u,d} X_{17}^{\mu} \bar{f} \gamma_{\mu} (g_{vf} + \gamma^5 \tilde{g}_{vf}) f. \tag{2}$$

All the relevant processes considered in this work are proportional to the coupling combination $(g_{ve}^2 + \tilde{g}_{ve}^2)$, up to terms involving the ratio $m_e^2/M_X^2 < 10^{-3}$, which will be neglected in the following. The dominant production mechanism for the X_{17} boson in the PADME experiment (regardless of its parity and spin nature) is from the resonant process $e^+e^- \to X_{17}$. For high-energy positrons impinging on the target electrons taken to be at rest,[1] the resonant condition reads

$$E_{\text{res}} = \frac{M_X^2}{2m_e}. \tag{3}$$

We assume that the positron energies E_+ have a Gaussian distribution with central value E and spread σ_E,[2]

$$f(E_+, E) = \frac{1}{\sqrt{2\pi}\sigma_E} e^{-\frac{(E_+ - E)^2}{2\sigma_E^2}}. \tag{4}$$

We will work under the assumption of that the energy distribution of the positrons in the beam can be considered continuous when compared to the X_{17} width Γ_X, which implies the following requirement:

$$\frac{\Gamma_X M_X}{2m_e} \frac{1}{\sigma_E} N_{\text{tot}}(E) \sim \left(\frac{N_{\text{tot}}(E)}{1 \times 10^7}\right) \left(\frac{g_{ve}}{2 \times 10^{-4}}\right)^2 \gg 1, \tag{5}$$

where for simplicity of notations in the case of electron couplings we have defined $g_{ve} \equiv \left[\sqrt{g_{vf}^2 + \tilde{g}_{vf}^2}\right]_{f=e}$. In Eq. (5) $N_{\text{tot}}(E)$ is the total number of positrons in the beam with nominal energy E, and the strong inequality holds for $\sigma_E \sim O(1)$ MeV.

At the leading order in QED, the resonant cross section for production of a vector X_{17} is given by

$$\sigma_{\text{res}}^{\text{Vect.}} = \frac{g_{ve}^2}{2m_e} \delta(E_+ - E_{\text{res}}). \tag{6}$$

The final number of X_{17} produced per positron on target for a given beam energy E is thus given by

$$\mathcal{N}_{X_{17}}^{\text{per poT}}(E) = \frac{\mathcal{N}_A Z \rho}{A} \ell_{\text{tar}} \frac{g_{ve}^2}{2m_e} f(E_{\text{res}}, E), \tag{7}$$

where ℓ_{tar} and ρ are, respectively, the target thickness and mass density. For resonantly produced X_{17} the boost factor is rather small, $\gamma_{X_{17}} = \frac{M_X}{2m_e} \sim 17$, implying that even for the smallest experimentally allowed couplings, X_{17} decays will occur promptly, with typical decay lengths never exceeding $O(1)$ cm.

The X_{17} particle mass is constrained by nuclear data to lay in the limited range given in Eq. (1), which suggests the range in which the beam energy should be varied in order to optimize the X_{17} search strategy. In this work we will consider a "conservative" strategy in which the beam energy is varied in the interval $E \in [265, 297]$ MeV, which corresponds to a scan in the center-of-mass (c.m.) energy range $\sqrt{s} \in [16.46, 17.42]$ MeV, that is, a 2σ range around the X_{17} mass hint as measured in ^{4}He. We will also show the projected sensitivity for a more "aggressive" search in which the beam energy is restricted to vary in the interval $E \in [273, 291]$ MeV, corresponding to $\sqrt{s} \in [16.72, 17.25]$ MeV, that is, a 2σ range around the X_{17} mass hint obtained using a naive combination (i.e., neglecting possible correlations) of the ^{4}He and ^{8}Be ATOMKI measurements [2,3].

The sensitivity of the scanning procedure depends on the energy step ΔE used in the scan. For a Gaussian beam energy distribution the number of produced X_{17} falls

[1]This is a very good approximation for all electrons in the $2s$, $2p$, and $1s$ atomic shells of ^{12}C [34,43].

[2]For positron energies $E_+ \sim 10$–20 MeV the typical energy loss in crossing a 100 μm diamond target is of the order of $O(100)$ keV. Typical values of the PADME beam spread σ_E are of $O(1)$ MeV, so distortion effects on the energy distribution can be neglected.

exponentially fast when the mean beam energy E departs from the resonance energy $E_{\rm res}$ and reaches a minimum when $|E - E_{\rm res}| = \Delta E/2$. Denoting by α the relative variation of the projected limit obtainable with the highest vs lowest production rates, the energy step ΔE can be determined in terms of α as

$$\Delta E \simeq 4\sigma_E\sqrt{\alpha}. \tag{8}$$

For the projections of the PADME Run III sensitivity discussed below, we require $\alpha \sim 20\%$. Finally, a useful approximation to the production rate of a vector X_{17}, which in our setup with a 100 μm diamond target holds to a few percent level, is given by

$$\mathcal{N}^{\rm Vect.}_{X_{17}} \simeq 1.8 \times 10^{-7} \times \left(\frac{g_{ve}}{2 \times 10^{-4}}\right)^2 \left(\frac{1\ \text{MeV}}{\sigma_E}\right), \tag{9}$$

where we have assumed that the beam energy is centered on the resonant energy $\sqrt{s} = M_X$.

In the case where the X_{17} is a pseudoscalar particle [axionlike particle (ALP)], the relevant Lagrangian is

$$\mathcal{L}^{\rm ALP} \supset \sum_{f=e,u,d} g_{af} m_f X_{17} \bar{f} \gamma^5 f. \tag{10}$$

The production cross section is given by [44]

$$\sigma^{\rm ALP}_{\rm res} = \frac{\pi m_e g^2_{ae}}{4} \times \delta(E_+ - E_{\rm res}). \tag{11}$$

Since photon couplings are independent of the initial and final state fermion chiralities, radiative corrections are similar to the case of a vector X_{17}. Thus, for the case of a pseudoscalar X_{17} produced by a positron beam tuned at the resonant energy and decaying into an electron-positron pair, we have

$$\mathcal{N}^{\rm ALP}_{X_{17}} \simeq 5.8 \times 10^{-7} \times \left(\frac{g_{ae}}{\text{GeV}^{-1}}\right)^2 \left(\frac{1\ \text{MeV}}{\sigma_E}\right). \tag{12}$$

When the X_{17} decays also into photons or into other dark sector particles, this result should be multiplied by $\text{BR}(X_{17} \to e^+e^-)$.

III. THE PADME EXPERIMENT RUN III

The DAΦNE BTF at LNF offers interesting prospects for a X_{17} search based on resonant production [34]. In particular, the LNF accelerator complex can provide a positron beam and vary its energy in the required range around 280 MeV. Assuming a typical diamond target (with an electron density of 10^{24} cm^{-3}) of 100 μm such as the one actually in use in the PADME experiment [41,42], several thousand X_{17} can be produced per 10^{10} positrons on target (POT).

For this reason the PADME experiment has planned dedicated data taking to search for X_{17} exploiting resonant production, called Run III. For this run, starting in the autumn of 2022, the detector has been optimized to measure X_{17} visible decays. Using the ECal instead of the charged particle veto to detect the electron positron pairs will allow PADME to reach a much stronger rejection of the beam related background with respect to Run II conditions. To suppress the photon background a new detector called ETag has been assembled. It is made of 5 mm thick bars of plastic scintillators covering the front face of the PADME ECal. Owing to the low Z of plastic scintillators and to their very small thickness, the bars will be sensitive only to charged particles, allowing one to separate photons from electrons and positrons.

As mentioned above, PADME plans to carry out a scan on various energy bins in order to thoroughly cover the interesting parameter space. Owing to the fact that the X_{17} width is much smaller than the beam energy spread $\Gamma_X \ll \sigma_E$, the X_{17} particle is expected to contribute to the measured $e^+e^- \to e^+e^-$ rate mostly in a single bin of the scan, the one in which $|M_{17} - \sqrt{s}|$ is minimum. Since the excess will occur within a single energy point, the remaining ones will directly measure the background, so the significance of the excess can be directly inferred from the data without appealing to any MC simulation.

As will be detailed in Sec. IV, according to the predicted signal and background rates that are summarized in Table I, the excess of electron-positron pairs due to X_{17} production/decay could be at the subpercent level. Quantifying precisely the confidence level of the exclusion limits (or of a detected excess in the signal) will thus require an extremely precise control on the acquired luminosity point by point. Measuring simultaneously, using ECal, the rate for the $e^+e^- \to e^+e^-$ and $e^+e^- \to \gamma\gamma$ processes will allow one to monitor the variation of their ratio, which is not affected by the previous uncertainty. This strategy drastically reduces systematic effects with respect to single measurements of the $e^+e^- \to e^+e^-$ rate since systematic errors related to both luminosity and acceptance measurements cancel in the ratio.

TABLE I. Expected number of background and signal events per 1×10^{10} positrons on target. The t-channel values before selection cuts correspond to $e^{\pm}$ with energies larger than 1 MeV. The acceptance cuts do not include the $\gamma\gamma$ tagging from the ETag. BG, background; Ev., events; Acc., acceptance; ch., channel.

BG process	No. of Ev.	No. of Ev. in Acc.	Acc.
$e^+e^- \to e^+e^-$ (t-ch.)	5.4×10^7	6.9×10^4	0.13%
$e^+e^- \to e^+e^-$ (s-ch.)	3.2×10^4	6.4×10^3	20%
$e^+e^- \to \gamma\gamma$	2.9×10^5	1.3×10^4	4.5%
$e^+e^- \to X_{17} \to e^+e^-$	1250	250	20%

We will present the projection for PADME Run III based on the following two scenarios for the total number of POT and the beam energy resolution.

(a) *Conservative*.—2×10^{11} total POT on target, a 0.5% beam spread, a broad energy range [265, 297], and an energy scan with 12 bins.

(b) *Aggressive*.—4×10^{11} total POT on target, a 0.25% beam spread, a narrower energy range [273, 291], and an energy scan with 14 bins.

In both cases, the number of steps were optimized based on the average projected limits. Note that the reach is only mildly reduced by further increasing the number of steps. Both scanning strategies are illustrated in Fig. 1, where a first estimate of the irreducible background level is also shown. The total number of positrons on target per energy point required is of the order of 10^{10}. Using ∼2500 positron on target per bunch, PADME will be able to collect the necessary statistics in a few days of fully efficient running. Reducing the beam spread σ_E implies that a larger number of energy steps must be used to cover the entire interesting region. For a fixed number of total positrons on target, the larger production rate per positron from Eq. (7) is therefore compensated for by the smaller number of positrons available for each energy point. However, as the number of background events is proportional to the number of impinging e^+, reducing the energy beam spread ultimately increases the signal-to-noise ratio in each energy bin, thus rising the sensitivity to signatures of NP and improving the projected experimental reach.

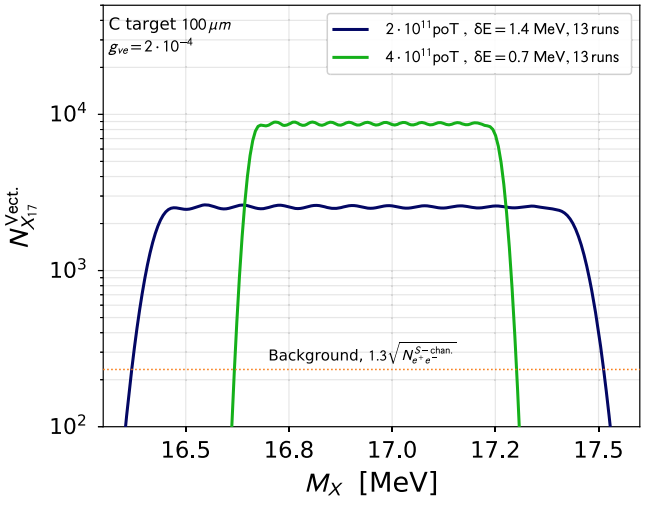

FIG. 1. Number of expected vector X_{17} as function of M_X, for the conservative (blue curve) and aggressive (dashed green) scanning configurations for $g_{ve} = 2 \times 10^{-4}$. The dotted orange line corresponds to the square root of the number of e^+e^- events from s-channel off-shell photons and illustrates the level of irreducible backgrounds.

IV. MAIN BACKGROUND PROCESSES

The use of resonant production offers a unique opportunity for enhancing the X_{17} production rates compared to the associated $e^+e^- \to \gamma X_{17}$ production. However, it also introduces challenging QED background sources which are hard to constrain. Given that the resonant production of X_{17} requires a low c.m. energy of ∼17 MeV, the main background sources are

(i) t- and s-channel Bhabha scattering,

(ii) $e^+e^- \to \gamma\gamma$,

(iii) $e^+N \to e^+N + \gamma$.

While Bhabha scattering is producing the same final state as X_{17} decays, the remaining processes produce at least one photon. In detectors using a pure calorimetric approach photons and electrons are indistinguishable, implying that a non-negligible background contribution from the photons' final state can arise. We will first concentrate on Bhabha scattering, assuming that photons background can be controlled by identifying photons in the final state, as will be discussed in the Sec. IV B. We will study the two Bhabha contributions separately to provide a better understanding of the physics at a fixed target, neglecting their interference term. The interference term has been checked to be negative and to produce a reduction of the total cross section below the percent level.

A. The Bhabha scattering background

The unique Standard Model (SM) process that can produce final states identical to the X_{17} decays at c.m. energies in the MeV range is $e^+e^- \to \gamma^* \to e^+e^-$, where γ^* denotes an off-shell photon. In the SM, Bhabha scattering proceeds via two different contributions—namely, the t-channel and s-channel amplitudes depicted in Fig. 2. While the final state is the same, their kinematic, especially in fixed target experiments, is very different. The t-channel process, despite being dominant in terms of contributions to the total cross section, can be efficiently rejected for having a quasielastic behavior, with the positron retaining almost all of its original energy and the electron remaining almost at rest (the green distribution in Fig. 3). This is a characteristic of the fixed target experiments in which the initial

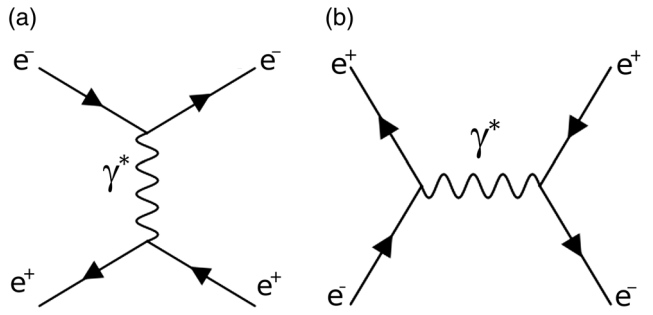

FIG. 2. (a) t-channel and (b) s-channel diagrams contributing to Bhabha scattering in the SM.

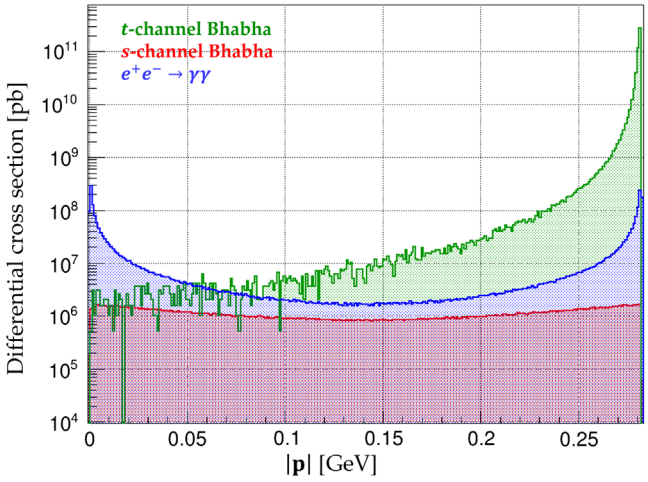

FIG. 3. Differential cross sections for the main sources of background as a function of the three-momentum of the outgoing positron and photon $|\mathbf{p}|$.

energy of the two particles is very different. Even when one exploits the different kinematics, the contribution of the t-channel process cannot be neglected. The s-channel process, on the other hand, has the same kinematics of the signal $e^+e^- \to X_{17} \to e^+e^-$ because the virtuality of the off-shell photon is $\sqrt{s} \sim M_X$. For this reason the s-channel process constitutes an irreducible source of background and represents the limiting factor for the sensitivity of experiments that exploit resonant production.

B. Photon background

In order to control the photon related background, a detector separating electron from photon clusters is required. For this reason, during Run III a new detector called ETag will be introduced into the original PADME setup. ETag will produce signals only if the crossing particle is electrically charged, with a few percent mistagging probability of identifying a photon as a charged particle.

The two photon annihilation process is the most relevant photon-based source of background due to the large cross section and the reduced effectiveness of the kinematical constraints. Assuming a mistagging probability $\epsilon_{\text{mis}} = 5\%$, a rejection factor on the $e^+e^- \to \gamma\gamma$ process of $1/\epsilon_{\text{mis}}^2 = 400$ can be obtained. Such a value, if achievable, would reduce the background originating from two photon annihilation to a negligible level.

Positron bremsstrahlung can also originate events with two charged particles if the radiated photon is mistagged as a charged particle and the two particles are entering the ECal acceptance. Both of these conditions are rare, with the process dominated by high-energy forward positrons and soft forward photons crossing the PADME ECal central hole. In addition, the two clusters eventually produced in the ECal will hardly reproduce the correct invariant mass value of 17 MeV. For this reason the background coming from bremsstrahlung can be considered negligible.

C. Beam related and pileup backgrounds

An additional possible source of background comes from overlapping beam-target interactions or beam related backgrounds. In the first case interactions of two different primary positrons can produce two simultaneous clusters in the PADME ECal. In the second case the interactions of the beam halo with beam line elements can produce multiple cluster events. These sources of background are proportional to the beam intensity, which will be reduced to a few thousand e^+/bunch in PADME Run III, a factor of 10 lower with respect to PADME Run II.

Combinatorial background sources can be controlled by applying several kinematic constraints to the event selection. The Bhabha kinematics is highly constrained so that the energy and the polar angle of each of the leptons are connected by an analytic expression, $E_{e^\pm} = f(\theta_{e^\pm})$. The following simple set of conditions can be applied to reject combinatorial backgrounds:

(i) $E_{e^+} + E_{e^-} = E_{\text{beam}}$,
(ii) $M^2(e^+e^-) = \sqrt{s}$,
(iii) $E_{e^\pm} = f(\theta_{e^\pm})$.

This strategy is well understood, and has been proven to be quite effective in the analysis of $e^+e^- \to \gamma\gamma$ events during PADME Run II [45].

D. Expected backgrounds summary

Let us now summarise the expected background contribution obtained by simulating final state kinematics with the CalcHEP package. We compute the total number of expected events using the cross section provided by CalcHEP, and we evaluate the acceptance adopting the following strategy:

(i) The energy of both outgoing particles E_1, E_2 is in the range: $E_{1,2} > 100$ MeV.
(ii) The azimuthal angle of both particles θ_1, θ_2 is in the range: $25.5 \lesssim \theta_{1,2}/\text{mrad} \lesssim 77$.

Applying these conditions, we find the number of signal and background events for each energy point of the scan ($\sim 1 \times 10^{10}$ POT). Our results are summarized in Table I. The signal rate has been obtained for $g_{ve} = 2 \times 10^{-4}$, which saturates the unexplored region of parameter space for vector particles. For the above background level, projected limits at 90% C.L. will thus correspond to having fewer than ~360 NP events.[3] Table I shows that the X_{17} production rate is non-negligible with respect to the background events for small values of the g_{ve}

[3]We assume that the $\gamma\gamma$ background will be reduced to a negligible level from the tagging in the ETag detector.

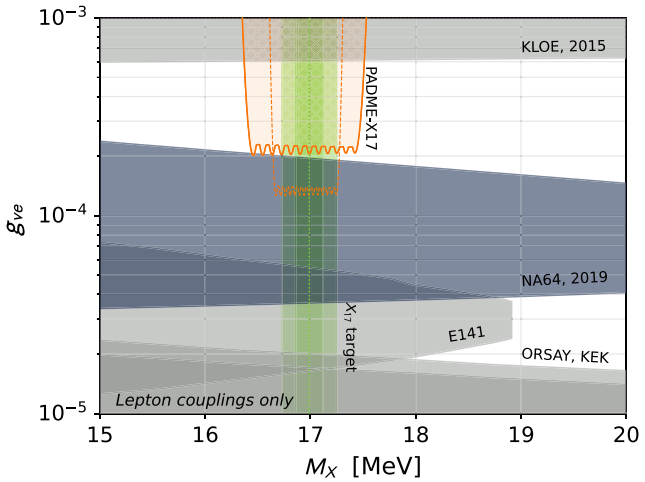

FIG. 4. Projected 90% C.L. sensitivity of PADME Run III on the g_{ve} coupling of a X_{17} vector boson for conservative (solid orange line) and aggressive (dashed orange line) setups. Lepton-based experimental limits from the KLOE [25], NA64 [24], E141 [17], KEK, and Orsay [21,22] experiments are also shown. The dark (light) green band represents the 1σ (2σ) X_{17} mass target from a naive combination of the ^{4}He and ^{8}Be ATOMKI results [2,3].

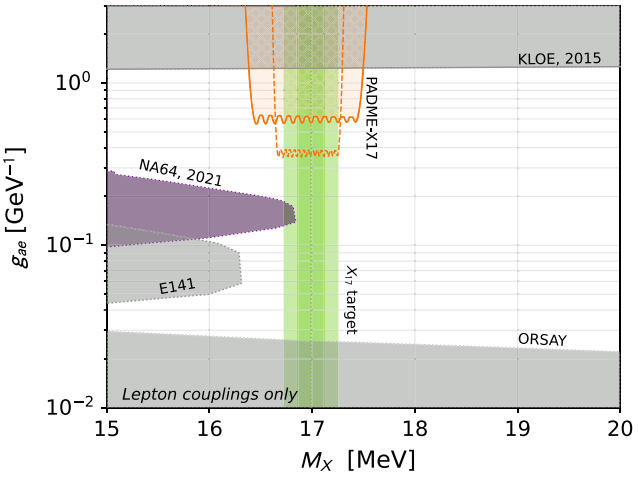

FIG. 5. Projected 90% C.L. sensitivity of PADME Run III on the g_{ae} coupling of a X_{17} ALP for conservative (solid orange line) and aggressive (dashed orange line) setups. Lepton-based experimental limits from the KLOE [25], NA64 [24], E141 [17], and Orsay [22] experiments are also shown. The dark (light) green band represents the 1σ (2σ) X_{17} mass target from a naive combination of the ^{4}He and ^{8}Be ATOMKI results [2,3].

coupling. The resulting signal acceptance has been obtained using the Bhabha s-channel kinematics, which is expected to be identical to the X_{17} one for prompt X_{17} decays. The actual acceptance value will depend on the final experimental cut strategy.

V. PROJECTIONS

In Fig. 4 we show the projections of the constraints on g_{ve} for the case of vector X_{17} as a function of its mass. For a vector particle with mass $M_X \approx 17$ MeV, the parameter space below $g_{ve} \approx 0.2 \times 10^{-3}$ is excluded by a combination of the E141 [17] and NA64 experiments [23], as well as by other beam dump experiments [21,22]. As can be seen in the figure, in the vector boson case the projected sensitivity of PADME Run III reaches all the way down to the upper limit from NA64, completely covering the still viable parameter space region. PADME Run III will thus exhaustively probe the hypothesis that the ATOMKI anomaly is due to a new vector boson with mass $M_X \approx 17$ MeV.

When the X_{17} is instead a spin-0 ALP, the existing limits are significantly less constraining due to the somewhat shorter lifetime and the slightly reduced production rate of an X_{17} ALP compared to a vector boson. In particular, we see in Fig. 5 that the NA64 limit [23] is barely reaching into the parameter space region favored by the nuclear experimental data. In contrast, the projections corresponding to the regions in orange indicate that PADME Run III will be able to probe a significant part of the viable parameter space for an X_{17} ALP.

VI. CONCLUSION

In this work we have described a novel approach to probing the existence of the putative X_{17} boson hinted at by the anomalies in the ^{8}Be and ^{4}He nuclear transitions reported by the ATOMKI Collaboration, and more generally of any new light boson with a mass close to 17 MeV and coupled to $e^{\pm}$. By exploiting the resonant annihilation of positrons of an energy-tuned beam on atomic electrons in a thin target, the scan-based procedure that we have described can be used to extract the signal while fitting the background directly from the off-resonance data.

We have studied the implementation of this strategy in the upcoming Run III of the PADME experiment at LNF. We have worked out a number of projections based on a statistic of a few $\times 10^{11}$ total positrons on target. We have considered only statistical errors on the signal and background. However, there are good reasons to expect that systematic errors could be kept to a similar level, including in particular the uncertainty on the relative number of positrons on target collected at each energy point of the scan. In this case several weeks of data taking at PADME would be sufficient to cover completely the parameter space region still viable for a spin-1 X_{17} candidate. In contrast, it will not be possible to completely exclude (or discover with certainty) a spin-0 X_{17} ALP, but still it will be possible to significantly reduce the viable parameter space. It is worth mentioning at this point that, since the remaining parameter space for an X_{17} ALP lies is the small coupling region, typical decay lengths can be as large as $\sim$1 cm. Hence, if a sufficiently precise vertexing of the decay could be engineered, the background would be

dramatically reduced, and eventually it might be possible to close also this region. While this work has focused on the mass range $M_X \in [16, 18]$ MeV determined by the BTF beam energy range, the same technique could be used in the future to probe all types of light bosons that feebly interact with $e^{\pm}$ with masses in the tens of MeV range, based on the availability of positron beams of adequate and tunable energies.

ACKNOWLEDGMENTS

We acknowledge several discussions with members of the PADME Collaboration, particularly P. Valente for fundamental inputs on the LNF beam setup and P. Gianotti for discussions on the details of the PADME experimental strategy. L. D. and E. N. have been supported in part by the INFN "Iniziativa Specifica" Theoretical Astroparticle Physics (TAsP-LNF). E. N. and M. R. are partially supported by the Sapienza Grant "Ricerca del bosone X17 nell'esperimento PADME ai laboratori Nazionali di Frascati." L. D. is supported by the European Union's Horizon 2020 research and innovation program under Marie Skłodowska-Curie Grant Agreement No. 101028626. M. M. acknowledges Professor A. D'Angelo for bringing him into contact with beyond Standard Model physics.

Note added.—Recently, a preprint composed by the ATOMKI Collaboration appeared that reports the observation of a further anomaly in the large angle correlation of e^+e^- pairs produced in ^{12}C nuclear transitions [46]. This new anomaly is consistent with the X_{17} vector boson interpretation of the ^{8}Be and ^{4}He anomalies, but it is at odds with an X_{17} of a pseudoscalar nature [5].

[1] A. J. Krasznahorkay *et al.*, Observation of Anomalous Internal Pair Creation in ^{8}Be: A Possible Indication of a Light, Neutral Boson, Phys. Rev. Lett. **116**, 042501 (2016).
[2] A. J. Krasznahorkay *et al.*, New results on the ^{8}Be anomaly, J. Phys. Conf. Ser. **1056**, 012028 (2018).
[3] A. J. Krasznahorkay, M. Csatlós, L. Csige, J. Gulyás, A. Krasznahorkay, B. M. Nyakó, I. Rajta, J. Timár, I. Vajda, and N. J. Sas, New anomaly observed in ^{4}He supports the existence of the hypothetical X17 particle, Phys. Rev. C **104**, 044003 (2021).
[4] X. Zhang and G. A. Miller, Can a protophobic vector boson explain the ATOMKI anomaly?, Phys. Lett. B **813**, 136061 (2021).
[5] J. L. Feng, T. M. P. Tait, and C. B. Verhaaren, Dynamical evidence for a fifth force explanation of the ATOMKI nuclear anomalies, Phys. Rev. D **102**, 036016 (2020).
[6] M. Viviani, E. Filandri, L. Girlanda, C. Gustavino, A. Kievsky, L. E. Marcucci, and R. Schiavilla, $X17$ boson and the $^3\mathrm{H}(p, e^+e^-)^4\mathrm{He}$ and $^3\mathrm{He}(n, e^+e^-)^4\mathrm{He}$ processes: A theoretical analysis, Phys. Rev. C **105**, 014001 (2022).
[7] J. R. Batley *et al.* (NA48/2 Collaboration), Search for the dark photon in π^0 decays, Phys. Lett. B **746**, 178 (2015).
[8] J. L. Feng, B. Fornal, I. Galon, S. Gardner, J. Smolinsky, T. M. P. Tait, and P. Tanedo, Protophobic Fifth-Force Interpretation of the Observed Anomaly in ^{8}Be Nuclear Transitions, Phys. Rev. Lett. **117**, 071803 (2016).
[9] J. L. Feng, B. Fornal, I. Galon, S. Gardner, J. Smolinsky, T. M. P. Tait, and P. Tanedo, Particle physics models for the 17 MeV anomaly in beryllium nuclear decays, Phys. Rev. D **95**, 035017 (2017).
[10] K. Ban, Y. Jho, Y. Kwon, S. C. Park, S. Park, and P.-Y. Tseng, Search for new light vector boson using J/Ψ at BESIII and Belle II, J. High Energy Phys. 04 (2021) 091.
[11] U. Ellwanger and S. Moretti, Possible explanation of the electron positron anomaly at 17 MeV in ^{8}Be transitions through a light pseudoscalar, J. High Energy Phys. 11 (2016) 039.
[12] D. S. M. Alves and N. Weiner, A viable QCD axion in the MeV mass range, J. High Energy Phys. 07 (2018) 092.
[13] D. S. M. Alves, Signals of the QCD axion with mass of 17 MeV/c^2: Nuclear transitions and light meson decays, Phys. Rev. D **103**, 055018 (2021).
[14] J. Backens and M. Vanderhaeghen, X17 Discovery Potential in the $\gamma N \to e^+e^-N$ Process at Electron Scattering Facilities, Phys. Rev. Lett. **128**, 091802 (2022).
[15] M. Hostert and M. Pospelov, Novel multilepton signatures of dark sectors in light meson decays, Phys. Rev. D **105**, 015017 (2022).
[16] W. Altmannshofer, J. A. Dror, and S. Gori, New insights into axion-lepton interactions, arXiv:2209.00665.
[17] E. M. Riordan *et al.*, Search for Short-Lived Axions in an Electron Beam Dump Experiment, Phys. Rev. Lett. **59**, 755 (1987).
[18] J. D. Bjorken, R. Essig, P. Schuster, and N. Toro, New fixed-target experiments to search for dark gauge forces, Phys. Rev. D **80**, 075018 (2009).
[19] S. Andreas, C. Niebuhr, and A. Ringwald, New limits on hidden photons from past electron beam dumps, Phys. Rev. D **86**, 095019 (2012).
[20] Y.-S. Liu and G. A. Miller, Validity of the Weizsäcker-Williams approximation and the analysis of beam dump experiments: Production of an axion, a dark photon, or a new axial-vector boson, Phys. Rev. D **96**, 016004 (2017).
[21] A. Konaka *et al.*, Search for Neutral Particles in Electron Beam Dump Experiment, Phys. Rev. Lett. **57**, 659 (1986).
[22] M. Davier and H. Nguyen Ngoc, An unambiguous search for a light Higgs boson, Phys. Lett. B **229**, 150 (1989).

[23] D. Banerjee *et al.* (NA64 Collaboration), Improved limits on a hypothetical $X(16.7)$ boson and a dark photon decaying into e^+e^- pairs, Phys. Rev. D **101**, 071101 (2020).
[24] Y. M. Andreev *et al.* (NA64 Collaboration), Search for pseudoscalar bosons decaying into e^+e^- pairs in the NA64 experiment at the CERN SPS, Phys. Rev. D **104**, L111102 (2021
[25] A. Anastasi *et al.*, Limit on the production of a low-mass vector boson in $e^+e^- \to U\gamma$, $U \to e^+e^-$ with the KLOE experiment, Phys. Lett. B **750**, 633 (2015).
[26] J. Balewski *et al.*, The DarkLight experiment: A precision search for new physics at low energies, arXiv:1412.4717.
[27] L. Doria, P. Achenbach, M. Christmann, A. Denig, and H. Merkel, Dark matter at the intensity frontier: The new MESA electron accelerator facility, Proc. Sci., ALPS2019 (**2020**) 022.
[28] N. Baltzell *et al.*, The heavy photon search experiment, arXiv:2203.08324.
[29] C. Hati, J. Kriewald, J. Orloff, and A. M. Teixeira, Anomalies in ^{8}Be nuclear transitions and $(g-2)_{e,\mu}$: Towards a minimal combined explanation, J. High Energy Phys. 07 (2020) 235.
[30] O. Seto and T. Shimomura, Atomki anomaly in gauged $U(1)_R$ symmetric model, J. High Energy Phys. 04 (2021) 025.
[31] T. Nomura and P. Sanyal, Explaining Atomki anomaly and muon $g-2$ in $U(1)_X$ extended flavour violating two Higgs doublet model, J. High Energy Phys. 05 (2021) 232.
[32] B. Dutta, S. Ghosh, and T. Li, Explaining $(g-2)_{\mu,e}$, the KOTO anomaly and the MiniBooNE excess in an extended Higgs model with sterile neutrinos, Phys. Rev. D **102**, 055017 (2020).
[33] A. Ghigo, G. Mazzitelli, F. Sannibale, P. Valente, and G. Vignola, Commissioning of the DAFNE beam test facility, Nucl. Instrum. Methods Phys. Res., Sect. A **515**, 524 (2003).
[34] E. Nardi, C. D. R. Carvajal, A. Ghoshal, D. Meloni, and M. Raggi, Resonant production of dark photons in positron beam dump experiments, Phys. Rev. D **97**, 095004 (2018).
[35] L. Marsicano, M. Battaglieri, M. Bondí, C. D. R. Carvajal, A. Celentano, M. De Napoli, R. De Vita, E. Nardi, M. Raggi, and P. Valente, Novel Way to Search for Light Dark Matter in Lepton Beam-Dump Experiments, Phys. Rev. Lett. **121**, 041802 (2018).
[36] L. Marsicano, M. Battaglieri, M. Bondí, C. D. R. Carvajal, A. Celentano, M. De Napoli, R. De Vita, E. Nardi, M. Raggi, and P. Valente, Dark photon production through positron annihilation in beam-dump experiments, Phys. Rev. D **98**, 015031 (2018).
[37] A. Celentano, L. Darmé, L. Marsicano, and E. Nardi, New production channels for light dark matter in hadronic showers, Phys. Rev. D **102**, 075026 (2020).
[38] M. Battaglieri *et al.*, Light dark matter searches with positrons, Eur. Phys. J. A **57**, 253 (2021).
[39] Y. M. Andreev *et al.*, Improved exclusion limit for light dark matter from e^+e^- annihilation in NA64, Phys. Rev. D **104**, L091701 (2021).
[40] M. Battaglieri *et al.*, Dark matter search with the BDX-MINI experiment, Phys. Rev. D **106**, 072011 (2022).
[41] M. Raggi and V. Kozhuharov, Proposal to search for a dark photon in positron on target collisions at DAΦNE Linac, Adv. High Energy Phys. (2014) 959802.
[42] M. Raggi, V. Kozhuharov, and P. Valente, The PADME experiment at LNF, EPJ Web Conf. **96**, 01025 (2015).
[43] E. Clementi and D. L. Raimondi, Atomic screening constants from scf functions, J. Chem. Phys. **38**, 2686 (1963).
[44] L. Darmé, F. Giacchino, E. Nardi, and M. Raggi, Invisible decays of axion-like particles: Constraints and prospects, J. High Energy Phys. 06 (2021) 009.
[45] F. Bossi *et al.* (PADME Collaboration), Cross-section measurement of two-photon annihilation in-flight of positrons at $\sqrt{s} = 20$ MeV with the PADME detector, arXiv:2210.14603.
[46] A. J. Krasznahorkay *et al.*, New anomaly observed in ^{12}C supports the existence and the vector character of the hypothetical X17 boson, Phys. Rev. C **106**, L061601 (2022).